Primate Biol., 3, 65–75, 2016
www.primate-biol.net/3/65/2016/
doi:10.5194/pb-3-65-2016

Primate Biology
Open Access

Lymphocryptovirus-dependent occurrence of lymphoma in SIV-infected rhesus macaques with particular consideration to two uncommon cases of non-Hodgkin's lymphoma

Antonina Klippert[1,*], Martina Bleyer[2,*], Ulrike Sauermann[1], Berit Neumann[1], Artur Kaul[3], Maria Daskalaki[1], Nicole Stolte-Leeb[1], Frank Kirchhoff[4], and Christiane Stahl-Hennig[1]

[1]Unit of Infection Models, German Primate Center, Goettingen, Germany
[2]Pathology Unit, German Primate Center, Goettingen, Germany
[3]Unit of Infection Biology, German Primate Center, Goettingen, Germany
[4]Institute of Molecular Virology, Ulm University Medical Center, Ulm, Germany
[*]These authors contributed equally to this work.

Correspondence to: Christiane Stahl-Hennig (stahlh@dpz.eu)

Received: 4 October 2016 – Revised: 29 November 2016 – Accepted: 29 November 2016 – Published: 20 December 2016

Abstract. Despite combination antiretroviral therapy, high-grade malignant non-Hodgkin's lymphoma (NHL) is still one of the most frequently acquired immunodeficiency syndrome (AIDS)-defining disorders in the end stage of infection with human immunodeficiency virus (HIV). NHL can also be observed in rhesus macaques infected with the simian immunodeficiency virus (SIV). Thus, they represent a useful model to study morphological characteristics and oncogenetic mechanisms of NHL in humans.

When reviewing the occurrence of lymphoma at the German Primate Center over the past 25 years within the context of pathogenic SIV infection we noticed a strikingly high incidence (four out of seven animals) of these tumors in rhesus macaques infected with ex vivo derived SIVmac251/32H/spleen in AIDS-defining end-stage disease. Polymerase chain reaction analysis of this virus stock revealed the co-presence of rhesus lymphocryptovirus (rhLCV), which represents the monkey homologue to human Epstein–Barr virus (EBV), suggesting an association between co-application of SIV and rhLCV and increased tumorigenesis.

In addition, we present two cases of NHL in rhesus macaques infected with a SIVmac239 *nef*-mutant variant because one exhibited an unusual immunophenotype and the other an uncommon organ manifestation. Histological and immunohistochemical examinations of tumors of the first animal revealed metastatic diffuse large *B*-cell lymphomas (DLBCL) affecting the stomach and the pancreaticoduodenal lymph nodes, of which the one in the stomach presented the rare dual expression of CD20 and CD3. Necropsy of the second animal revealed an obstructive DLBCL around the urinary bladder neck that led to urine backflow and eventually death due to acute uremia without any further AIDS-like manifestations. In the tumors of both animals, abundant Epstein–Barr nuclear antigen-2 expression was demonstrated, thus verifying concurrent rhLCV infection. Flow cytometric analyses revealed a high percentage of activation as well as proliferation in *B* cells from peripheral lymph nodes in both animals. Moreover, $CD4^+$ *T* cells were depleted in blood, colon and lymphoid tissue. Concomitantly, $CD8^+$ *T* cells showed an exhausted phenotype. The two case reports and the increased incidence of NHL following co-application of SIV and rhLCV underline the role of rhLCV in lymphomagenesis.

Published by Copernicus Publications on behalf of the Deutsches Primatenzentrum GmbH (DPZ).

1 Introduction

Lymphomas are linked to human immunodeficiency virus (HIV) infection in that they are known to occur in association with acquired immunodeficiency syndrome (AIDS) and are therefore classified as an AIDS-defining disease. Lymphoid neoplasms can be divided into Hodgkin's and non-Hodgkin's lymphomas (NHL). Most of the AIDS-associated lymphomas are high-grade malignant NHL of *B*-cell origin, and co-infection with Epstein–Barr virus (EBV) is assumed to play an important role in oncogenesis (Hamilton-Dutoit et al., 1993). Usually, *B* cells are latently infected with EBV, resulting in a lifelong asymptomatic state. In immunosuppressed individuals, virus reactivation is associated with the development of tumors. The World Health Organization (WHO) issued a new lymphoma classification in 2008 and developed a more detailed characterization of *B*-cell lymphomas based on morphology, immunophenotype and molecular findings as well as clinical features (Swerdlow et al., 2008). The most common NHL type according to this classification is the diffuse large *B*-cell lymphoma (DLBCL), accounting for 31 % of all NHLs (Armitage and Weisenburger, 1998).

Simian immunodeficiency virus (SIV) infection of rhesus macaques (*Macaca mulatta*) models that of human HIV infection with comparable pathogenic features such as $CD4^+$ *T*-cell loss and the development of AIDS-like symptoms (Phillips et al., 2014). NHL also develops during late-stage SIV infection and shares similar characteristics with HIV-associated NHL (Kahnt et al., 2002; Habis et al., 1999; Matz-Rensing et al., 1999). Concomitantly, these tumors are reported to be associated with rhesus lymphocryptovirus (rhLCV) infection, a herpesvirus closely related to EBV (Blaschke et al., 2001; Kahnt et al., 2002; Habis et al., 2000).

So far, reports evaluating the incidence of lymphoma depending on the used SIV challenge stocks are not available. Some authors describe the overall incidence of lymphoma development in cohorts of rhesus macaques ranging between 4 and 19 % (Habis et al., 1999; Kahnt et al., 2002) but associations with different SIV stocks are missing. Our report describes the relation between differently prepared SIVmac stocks and the incidence of lymphoma at the German Primate Center over the last 25 years. In addition, we present two cases of NHL in SIV-infected rhesus macaques, one because of its unusual location and the other because of its rare immunophenotype.

2 Material and methods

2.1 Ethical statement

The monkeys were housed at the German Primate Center under standard conditions complying with § 7–9 of the German Animal Welfare Act, which strictly adheres to the European Union guidelines (EU directive 2010/63/EU) on the use of non-human primates for biomedical research. Experienced veterinarians and animal caretakers constantly monitored the monkeys. An external ethics committee of the Lower Saxony State Office for Consumer Protection and Food Safety (LAVES) approved the experiments. A scoring system with defined endpoint guidelines was used for each animal.

2.2 Animals

This study comprised 165 rhesus macaques infected with SIVmac; 163 animals were included in the evaluation of SIV stock-dependent incidence of lymphoma. The selection criterion for this cohort was euthanasia because of early AIDS-defining illness as described (Siddiqui et al., 2009).

The two remaining animals are presented as case reports of SIV-associated lymphomas and were infected with a SIVmac239 *nef* mutant. Animal 1 (6.5 years, female) had to be euthanized due to AIDS-related symptoms at week 73 post-infection (pi). A complete necropsy with detailed gross evaluation was performed. Tissue samples from a broad organ spectrum including tumorous lesions were collected and placed in 10 % phosphate buffered formaldehyde.

Animal 2 (5.5 years, male) died unexpectedly at week 45 pi. Besides mild gastrointestinal symptoms, the animal did not show overt clinical signs prior to death. Tissue samples were processed as described for animal 1.

Flow cytometric data from the two case report animals were compared with those of seven other rhesus macaques infected in parallel with SIVmac239 ($n = 3$), SIVmac239 *nef* mutant ($n = 1$) or SIVmac239 *vpr* mutant ($n = 3$), without developing lymphoma up to 18 months after infection.

2.3 Sample collection and isolation of cells

Sampling of blood, lymph nodes and mononuclear cells (MNCs) from lymph nodes by fine-needle aspiration before and after the experimental SIV infection was performed as previously described (Klippert et al., 2015). As reported, colonic biopsies were collected and MNCs isolated (Schultheiss et al., 2011).

Blood samples, a peripheral lymph node and tissue from the colon were taken from animal 1 during necropsy. The lymphoid and colon tissues were placed in RPMI1640 medium (PAN-Biotech, Aidenbach, Germany) on ice enriched with 10 % fetal bovine serum (FBS) Gold (PAA, Pasching, Austria) and 1 % penicillin, 1 % streptomycin (both PAN-Biotech), 1 % gentamycin (Life Technologies GmbH, Darmstadt, Germany), 50 µg mL^{-1} neomycin (Roth, Karlsruhe, Germany), 100 U mL^{-1} nystatin (Roth) and 2.5 µg mL^{-1} amphotericin B (PAN-Biotech). MNCs from lymph nodes were obtained by forcing the tissue through 100 µm cell strainers (BD Falcon, Heidelberg, Germany). After two washing steps, cells were counted by trypan blue staining. MNCs from intestinal tissue were isolated as reported earlier (Schultheiss et al., 2011).

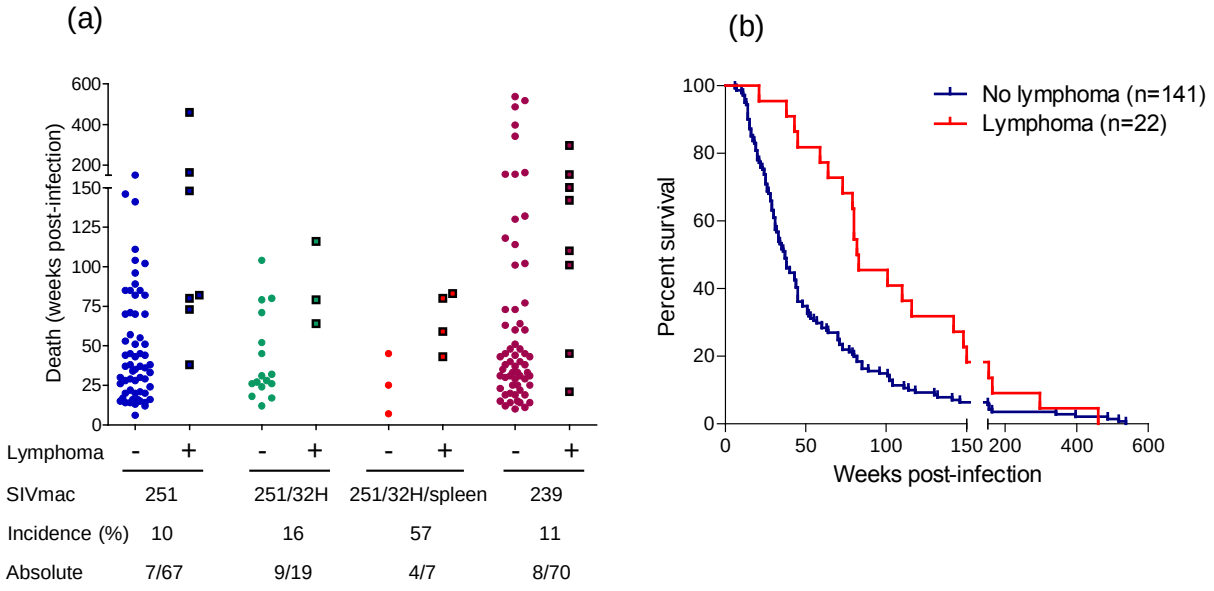

Figure 1. **(a)** Lymphoma incidence related to the utilized simian immunodeficiency virus stock. Each animal is depicted as an individual symbol. On the x axis, the occurrence of lymphoma is indicated by $+$ and $-$ in relation to the virus used for infection. Incidences of lymphoma cases in percent and the ratios of absolute numbers of lymphomas to number of animals included are given below. The y axis indicates survival time as weeks post-infection. Animals were euthanized with early AIDS-like symptoms. **(b)** Survival of monkeys infected with the different SIV stocks and sacrificed with early AIDS-defining disease without versus those with lymphoma development. Macaques euthanized with lymphomas survived on average longer than those without ($p < 0.0001$, Gehan–Breslow–Wilcoxon test).

Immunological and virological analyses for animal 2 were performed in blood and lymph node 1 week before death and in colon biopsies at 36 pi.

2.4 Flow cytometry and cell analysis

Whole blood (50 µl) or 2.5–5 $\times$ 10^5 enriched mononuclear cells from lymph nodes or colon were stained at room temperature in the dark with mixtures of pretitrated monoclonal antibodies (mAb) for 30 min. These included CD3 (AlexaFluor700, clone SP34-2), CD80 (PE, clone L307.4), CD4 (V450, clone L200), CD45 (V500, clone D058-1283) and Ki67 (PerCP-Cy5.5, clone B56), all from BD Biosciences, Heidelberg, Germany, and CD20 (PE-Cy7, clone 2H7), CD10 (APC-Cy7, clone HI10a), PD-1 (PE-Cy7, clone EH12.2H7) from BioLegend (San Diego, CA, USA), and CD8 (Pacific Orange; clone 3B5 from Beckman Coulter, Krefeld, Germany, or APC-Cy7; clone SK1 from BioLegend). Lysis of residual red blood cells (RBC) and fixation were performed through incubation with 1 mL RBC lysis/fixation solution (BioLegend) for 15 min. Following a washing step, cells were acquired by a LSR II cytometer (BD Bioscience), and analysis was performed with the help of FlowJo 9.6 software (Treestar, Ashland, OR, USA).

2.5 Histology and immunohistochemistry (IHC)

After fixation for at least 48 h, tissue samples of various organs and of grossly visible neoplastic lesions were paraffin-embedded, sectioned at 3 µm and stained with hematoxylin and eosin (HE) for histopathological examinations.

Immunophenotyping of lymphocytic tumors was performed by immunohistochemical staining of paraffin-embedded sections using an anti-CD3 antibody labeling *T* cells (Dako Deutschland GmbH, Hamburg, Germany, polyclonal rabbit anti-human CD3, 1 : 50) and an anti-CD20 antibody labeling *B* cells (Dako Deutschland GmbH, Hamburg, Germany, monoclonal mouse anti-human CD20cy, clone L26, 1 : 300). To determine the proliferative activity in neoplastic tissue, anti-Ki67 antibody (Dako Deutschland GmbH, Hamburg, Germany, monoclonal mouse anti-human Ki67 antigen, clone MIB-1, 1 : 50) was also applied as a primary antibody. Anti-Epstein–Barr nuclear antigen-2 (EBNA-2) antibody (Abcam, Cambridge, United Kingdom, clone PE2, 1 : 10) was used to analyze the presence of lymphocryptovirus in neoplastic cells (Kahnt et al., 2002).

IHC was performed with an automated immunostaining system (Discovery XT, Roche Diagnostics GmbH, Mannheim, Germany) using the SABC (streptavidin–biotin complex) method and DAB (diaminobenzidine tetrahydrochloride) for signal detection (DAB Map Kit, Roche Diagnostics GmbH, Mannheim, Germany). Rhesus lymph node or lymphoma tissue from a rhesus macaque with confirmed

rhesus lymphocryptovirus infection served as positive controls. Pure antibody diluent was applied to the negative control sections.

2.6 Real-time quantitative reverse transcription polymerase chain reaction (RT-qPCR) for the quantification of SIV

Quantification of the plasma viral load for SIV was carried out as previously described (Klippert et al., 2015).

2.7 DNA extraction and PCR for the detection of LCV

The SIVmac251/32H/spleen stock was analyzed for the copresence of LCV. For this purpose, total DNA was prepared from 0.2 mL of the virus stock using the First-DNA all-tissue kit (GEN-IAL GmbH, Germany) according to the manufacturer's instructions. A pan-herpesvirus consensus PCR targeting the DNA polymerase gene was carried out in a nested format (Chmielewicz et al., 2003) using 0.1 µg of extracted total DNA. The amplicon was purified and sequenced according to standard techniques. The obtained amplicon sequence was analyzed by NCBI BLAST search.

3 Results

3.1 Incidence of lymphoma development in relation to the used challenge virus

A total of 163 SIV-infected rhesus macaques were included to calculate the incidence of lymphoma development in SIV-infected rhesus macaques at the German Primate Center over the past two and a half decades. It should be noted that this report includes only macaques that were euthanized with early AIDS-defining illness. The animals were infected with different cell-free strains of SIVmac, i.e., 251, 239, 32H and 251/32H/spleen. SIVmac251 and SIVmac239 represent the two prototypes of SIV from macaques (Daniel, 1985). SIVmac215/32H was derived from an in vivo titration of SIVmac251 (Rud et al., 1994). SIVmac251/32H/spleen had been prepared as a homogenate from a spleen of a SIVmac251/32H-infected monkey without any in vitro passage (Dittmer et al., 1995). Details about the cohort are given in Table 1.

As shown in Fig. 1a, 7 of 67 animals infected with SIVmac251 developed lymphoma, accounting for an incidence of 10 %. Infection with SIVmac239 yielded a comparable incidence with 8 of 70 animals with lymphoid tumors. For the rhesus macaques infected with SIVmac251/32H, the incidence was about the same (16 %) with a total of 3 of 19 animals affected by lymphomas. The incidence was significantly higher in the animals infected with SIVmac251/32H/spleen (57 %) with four out of seven animals developing lymphoid tumors ($p = 0.0057$, Fisher's exact test) compared to the total of the other three groups.

Animals presenting with lymphoma at the time of euthanasia survived the infection on average longer than those without (median survival without lymphoma is 37 wpi and with lymphoma is 82.5 wpi; $p < 0.0001$, Gehan–Breslow–Wilcoxon test; Fig. 1b). Lymphomas thus developed mainly after a prolonged time of infection and immunosuppression and this was independent of the infecting SIV (data not shown). In contrast, the occurrence of lymphomas was not biased by sex ($p = 1$, Fisher's exact test), the inoculation route ($p = 0.6$ for intravenous and tonsillar route, $p = 0.1$ for intrarectal infection, Fisher's exact test), the source (DPZ and LABS: $p = 0.4$; DSTL: $p = 0.18$; CPRC: $p = 1$, Fisher's exact test) or the age at the time of infection ($p > 0.38$, Fisher's exact test).

3.1.1 Detection of LCV in the SIVmac251/32H/spleen virus stock

Since we suspected the spleen-derived SIV stock to contain lymphocryptovirus, a pan-Herpes virus PCR was performed with the cell-free SIV-containing fluid and the DNA sequence of the amplicon determined. A comparison of the 175 base pair DNA sequence with published sequences of lymphocryptovirus from macaques revealed 99 % identity to the published genome of the *Cercopithicine herpesvirus 15*, strain LCL8664 (accession no. AY037858.1). Thus, the SIVmac251/32H/spleen stock contained not only SIV but also rhesus lymphocryptovirus DNA.

3.2 Two case reports of lymphoma

3.2.1 Clinical signs, percentages of *T*- and *B*-cell subpopulations and plasma viral load

Here, we report about an in-depth analysis of two special cases of lymphomas in animals originating from the DPZ breeding colony and infected with a *nef* mutant of SIVmac239. Animal 1 suffered from persistent diarrhea with reduced food intake and 15 % weight loss. According to our scoring system, the animal was euthanized. Animal 2 showed a transient mild diarrhea and a slightly reduced appetence and died without any apparent clinical AIDS-defining illness. Both animals revealed a profound loss of $CD4^+$ cells in blood, lymphoid and colon tissue as indicated by percent difference to CD4 pre-infection values at or shortly before death (Fig. 2a). Due to the sudden death of animal 2, data from 1 to 9 weeks prior to necropsy were analyzed. In line with this, both animals had a high plasma viral load at or shortly before death (animal 1: 2.03×10^6 viral RNA copies mL^{-1} plasma; animal 2: 1.11×10^6 viral RNA copies mL^{-1} plasma).

$CD20^+$ *B* cells from lymph nodes were investigated for activation (CD80 expression) and proliferation (intranuclear Ki67) and compared to those of seven SIV-infected animals that did not develop a lymphoma. Both parameters were upregulated on or in *B* cells in the two groups over time, but

Table 1. Baseline characteristics of the SIV-infected rhesus macaques (*Macaca mulatta*) of Indian origin except for the two case reports.

Infecting virus	SIVmac251	SIVmac251/ 32H	SIVmac251/ 32H/spleen	SIVmac239
Number of macaques	67	19	7	70
Sex				
Male	60 (89 %)	11 (58 %)	3 (43 %)	58(83 %)
Female	7 (11 %)	8 (42 %)	4 (57 %)	12 (17 %)
Source*				
DPZ	28 (42 %)	17 (89.5)	7 (100 %)	31 (44 %)
CPRC	2 (3 %)	2 (10.5 %)		6 (8.5 %)
MIC	23 (34 %)			20 (29 %)
DSTL	14 (21 %)			13 (18.5 %)
Route of infection				
Intravenous	38 (57 %)	19 (100 %)	7 (100 %)	35 (50 %)
Intrarectal	18 (27 %)			
Tonsillar	11 (16 %)			35 (50 %)
Median age (year) at infection (minimum-maximum)	3.9 (2.1–16.9)	3.8 (2.0–15)	3.7 (2.4–7.3)	3.9 (2.2–15)

Abbreviations: DPZ is German Primate Center, Germany; CPRC is Caribbean Primate Research Center, Puerto Rico; MIC is Morgan Island Colony, USA; DSTL is Defence Science and Technology Laboratory, GB. The rhesus macaques of the DPZ originated from the CPRC, MIC, and the Centre de Primatologie, France.

Table 2. Percentage of expression of different surface and intracellular markers in SIV-associated NHL based on immunohistochemistry.

Animal	Tumor localization	CD3	CD20	Ki67	EBNA2
		expression in %			
1	Stomach	80–90	80–90	> 90	70–80
1	Lymph node	5–15	> 95	> 90	> 90
2	Urinary bladder	15–25	> 95	> 90	60–70

Abbreviations: SIV is simian immunodeficiency virus; NHL is non-Hodgkin's lymphoma; EBNA2 is Epstein–Barr nuclear antigen 2.

a higher expression was observed in the two lymphoma animals from week 14 post-infection onwards (Fig. 2b, left and middle panel). Concurrently, cytotoxic $CD8^+$ *T* cells from lymph nodes showed an upregulation of PD-1, a marker for exhaustion, but also for activation (Fig. 2b, right panel).

3.2.2 Gross pathology

Animal 1 revealed an ulcerated tumorous thickening of the gastric body wall measuring approximately 2 cm in diameter (Fig. 3a). Adjacent pancreaticoduodenal lymph nodes were severely enlarged.

Major gross findings in animal 2 were observed in the urogenital tract. There was bilateral hydroureter (diameter 0.5 mm) and bilateral hydronephrosis with moderate atrophy of the renal cortex and medulla. A large tumorous white mass (approximately $5 \times 4 \times 3.5$ cm) was visible in the wall of the urinary bladder. It was located in the region of the bladder neck and involved the orifices of both ureters leading to almost complete urethral obstruction (Fig. 3b).

3.2.3 Histology and immunohistochemistry

Histopathological examination of the gastric body mass of animal 1 revealed a densely cellular, infiltrative, unencapsulated, poorly demarcated round cell neoplasm composed of sheets of medium-sized to large neoplastic lymphocytes separated by a collagenous stroma. Tumor cells had indistinct cell borders with a small amount of finely granular eosinophilic cytoplasm. Nuclei were irregularly round, often indented, vesicular and revealed one to three prominent nucleoli. There was mild anisokaryosis and anisocytosis of the centroblastic tumor cells. The mitotic rate ranged from 6 to 10 per high power field (HPF). There were multifocal aggregates of infiltrating and residual small mature lymphocytes throughout the neoplasm (Fig. 4a). Infiltrative tumor growth led to focally extensive effacement of the gastric mucosa. The tumor extended into the outer muscular layer with occasional evidence of tumor cells in the gastric serosa. Immunohistochemically, the tumor cells equally expressed CD3 and CD20 (Fig. 4b and c, Table 2). While a small amount of tumor cells were only positive for CD3 or CD20, the majority of neoplastic lymphocytic cells expressed both CD3

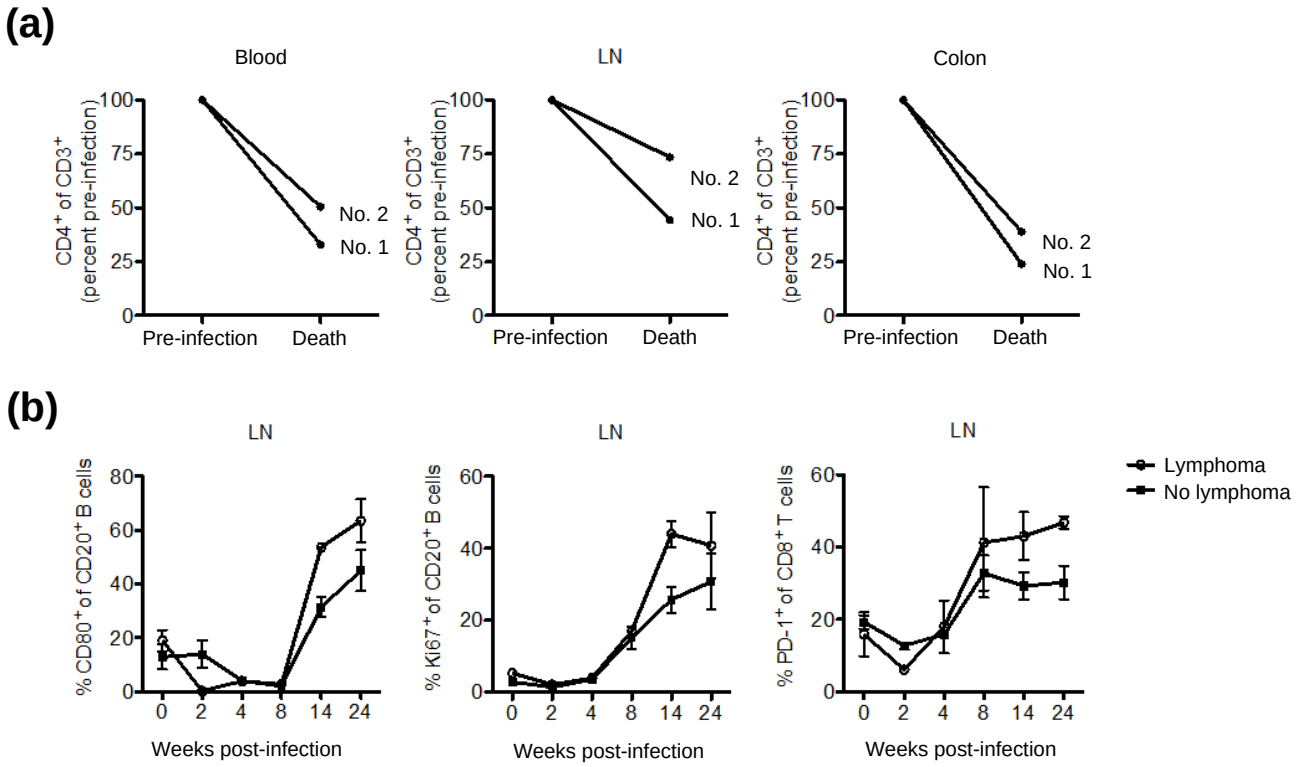

Figure 2. Percentages of *T* helper cell populations in blood as well as lymphoid and mucosal tissue of the two lymphoma case reports and those of activated lymph node *B* and *T* cells compared with animals infected with SIV concurrently but without development of lymphoma over time. **(a)** Proportion of $CD4^+$ *T* cells of $CD3^+$ cells normalized to pre-infection values in blood, lymph node and colon determined shortly before or at death (upper row). In each graph individual animal values designated nos. 1 and 2 and indicating the lymphoma case reports are shown. Pre-infection values of blood represent the mean of four independent measurements. For lymph node analysis one baseline value was available from a complete lymph node. Baseline values of the colon represent the mean of two independent analyses. **(b)** Longitudinal analysis of percentages of $CD80^+$ and $Ki67^+$ *B* cells, as well as PD-1^+ $CD8^+$ *T* cells in lymph nodes. Values from the two case report animals were compared with those from seven animals simultaneously infected with SIV. Post-infection measurements were conducted either with cells from whole lymph node at weeks 2 and 24 or with FNA cells at the other time points indicated. Pre-infection indicates values raised before infection; LN, lymph node.

and CD20. The enlarged pancreaticoduodenal lymph nodes revealed a comparable lymphocytic proliferation, which obscured normal lymph node architecture and extended into the perinodal adipose tissue. However, there were less mature lymphocytes and fewer amounts of collagenous stroma within the neoplastic tissue, and compared to the gastric neoplasm tumor cells were slightly larger (Fig. 4d). Almost all lymphocytic cells of the nodal tumor expressed CD20 admixed with only few CD3 positive cells (Fig. 4e and f, Table 2). In both tumors of animal 1, the majority of cells showed nuclear expression of Ki67, confirming the high proliferative activity of the lymphocytic neoplasms.

The tumorous mass in the urinary bladder neck region of animal 2 was represented by an unencapsulated neoplasm composed of sheets of round cells accompanied by a sparse collagenous stroma. Neoplastic cells were medium-sized to large and had variably distinct borders, scant amounts of eosinophilic granular cytoplasm and round to oval vesicular nuclei with one to three distinct nucleoli compatible with centroblasts. There was mild anisocaryosis and anisocytosis. The mitotic rate averaged five to seven per HPF (Fig. 5a). The neoplastic lesion led to effacement of the luminal mucosa, showed transmural expansion and infiltrated the caudal segments of the seminal vesicles (Fig. 5b). Almost all lymphocytic cells of the bladder tumor expressed CD20 and Ki67 (Fig. 5c, Table 2). Only a few CD3 positive cells could be observed within the tumor of animal 2 (Table 2).

Based on the histological appearance together with the immunophenotype and Ki67 expression, the tumor of animal 2 was diagnosed as a centroblastic DLBCL according to the WHO lymphoma classification. In animal 1, immunophenotyping and histological features of the nodal tumor were also compatible with a centroblastic DLBCL. In contrast, final diagnosis for the gastric neoplasm remained questionable due to the extensive expression of CD3 in this tumor. CD3 expressing lymphocytic cells partly represented infiltrating non-neoplastic *T* cells, especially in the periphery of the tumor, but there were also a considerable number of neoplastic

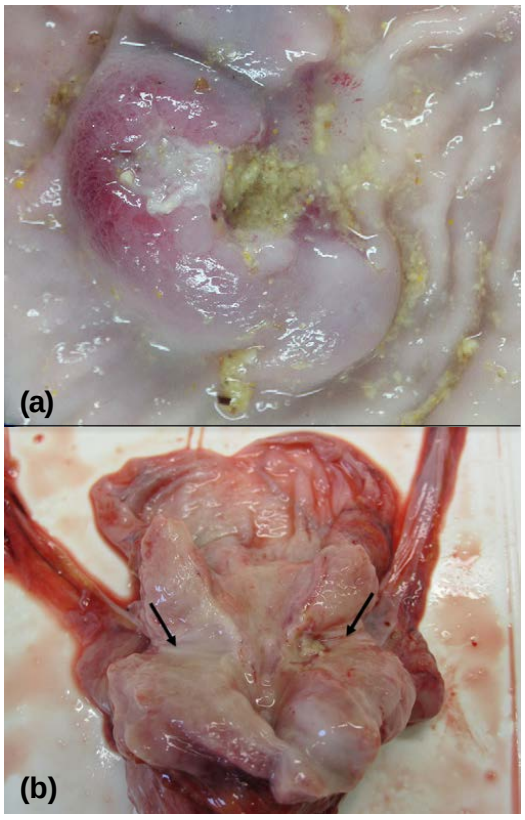

Figure 3. Gross findings in animals 1 and 2. **(a)** Mucosal surface of the opened stomach of animal 1 with a focal tumorous mass in the gastric wall is shown. **(b)** In animal 2 an extensive white tumorous mass was present in the bladder neck region obstructing the ureters in their orifice regions (arrows).

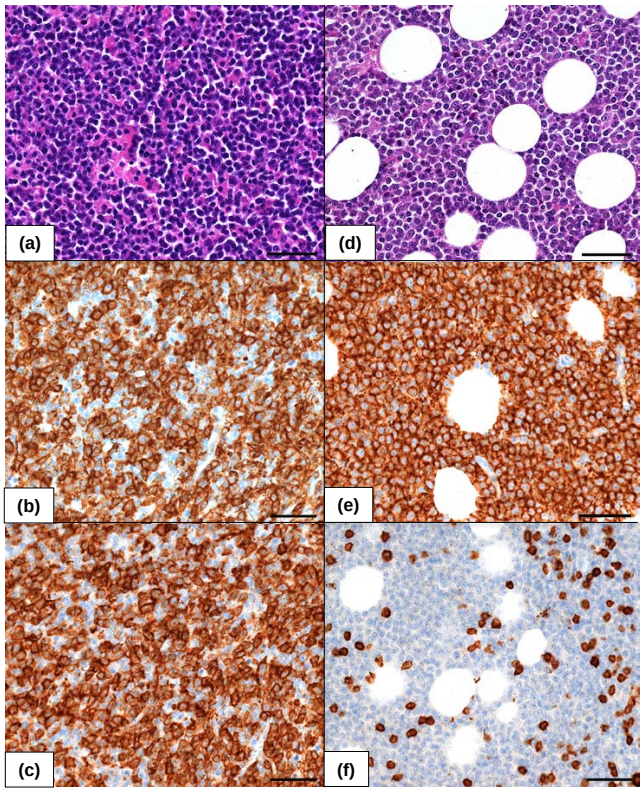

Figure 4. Light microscopic images of the gastric (**a**–**c**) and nodal tumor (**d**–**f**) of animal 1. **(a)** Neoplasm in the gastric wall is composed of densely cellular sheets of medium-sized to large lymphocytic round cells admixed with infiltrating and residual small mature lymphocytes. **(b)** Membranous co-expression of CD20 and **(c)** CD3 in the majority of lymphocytic neoplastic cells is shown. **(d)** The DLBCL in the pancreaticoduodenal lymph node is composed of monomorphic medium-sized to large tumor cells with rare mature lymphocytes and sparse collagenous stroma. **(e)** Almost all lymphocytic cells expressed CD20. **(f)** CD3 was only expressed by a small fraction of cells. HE staining (**a**, **d**); IHC with SABC method and chromogen DAB (**b**, **c**, **e**, **f**); scale bar = 50 µm. HE is hematoxylin and eosin; IHC is immunohistochemistry; SABC is streptavidin–biotin complex; DAB is diaminobenzidine tetrahydrochloride.

lymphocytic cells co-expressing both CD3 and CD20. However, as this neoplasia most likely represents a metastatic disease, the gastric tumor may also be classified as a DLBCL, but with aberrant co-expression of CD3.

EBNA-2 expression was present in all examined tumors indicating co-infection with rhLCV in both animals (Fig. 5d, Table 2).

4 Discussion

First, we analyzed the incidence of SIV-associated lymphoma in relation to the infecting virus stock. The highest incidence of lymphoma was observed after infection with the ex vivo prepared SIVmac251/32H/spleen stock leading to lymphomagenesis in almost 60 % of the macaques. When using the viruses SIVmac251, SIVmac239 or SIVmac32H for infection of rhesus macaques, we found lower incidences ranging between 10 and 16 %, similar to those reported by others. These overall incidences of lymphoma in cohorts of SIV-infected rhesus macaques varied between 4 % (Habis et al., 1999) and 19 % (Matz-Rensing et al., 1999; Kahnt et al., 2002). A detailed association of lymphoma development in relation to the infecting virus has not been performed in those studies. The high incidence of lymphoma linked to infection with our SIVmac251/32H/spleen stock was striking and also significant when compared to the total of the other groups. This virus stock was derived from a tissue homogenate prepared from the spleen of an adult SIV-infected monkey without any in vitro culture (Dittmer et al., 1995). As it is well known that almost all macaques older than 2 years of age are latently infected with lymphocryptovirus (Fujimoto and Honjo, 1991; Wang, 2013), we therefore suspected the co-presence of this virus in our SIV stock. Homogenization of the spleen could have released not only SIV from *T* cells but also rhLCV from *B* cells. Indeed, PCR anal-

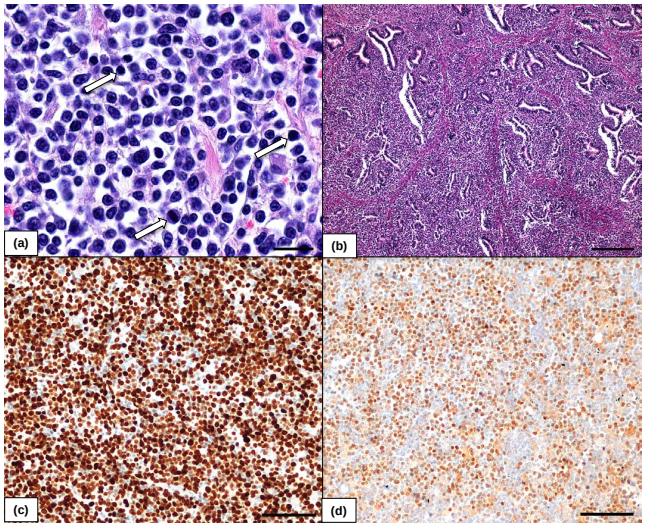

Figure 5. Light microscopic images of the urinary bladder tumor of animal 2. **(a)** DLBCL in the neck region of the urinary bladder composed of densely cellular sheets of medium-sized to large round cells exhibiting several mitoses (arrows) and **(b)** infiltrating the seminal vesicles. **(c)** Almost all tumor cells show nuclear expression of Ki67 and **(d)** the majority of neoplastic cells express EBNA2. HE staining (**a**, **d**); IHC with SABC method and chromogen DAB (**c**, **d**); scale bar is 20 µm **(a)**, 200 µm **(b)** and 100 µm (**c**, **d**). DLBCL is diffuse large *B*-cell lymphoma; EBNA2 is Epstein–Barr nuclear antigen 2; IHC is immunohistochemistry; HE is hematoxylin and eosin; SABC is streptavidin–biotin complex; DAB is diaminobenzidine tetrahydrochloride.

ysis and the following sequence comparison confirmed our assumption. Consequently, co-administration of rhLCV with immunosuppressing SIV might have either led to superinfection of the probably rhLCV-infected animals or re-activated the latent rhLCV infection. This could have resulted in an increased risk of accumulating genetic changes in growth-related genes, ultimately promoting and leading to malignant lymphomagenesis as previously hypothesized (Rivailler et al., 2004). However, the exact mechanisms of a boosted tumor development still remain elusive.

In addition, we focused on two cases of lymphoma in chronic SIV infection because they were special with respect to either the localization or the phenotype. Both animals presenting with tumorous masses had the co-infection with oncogenic rhLCV in common. Similarly, $CD4^+$ *T* cells were low in blood, lymphoid and mucosal tissue at the time of euthanasia or before death. These are well-known indicators of immunosuppression during SIV infection. Furthermore, we investigated complementary parameters such as activation and proliferation markers for *B* cells in the setting of lymphoma development. *B* cells from the two animals showed a considerably higher upregulation of CD80 and Ki67 in the lymphoid system compared to a cohort of animals concurrently infected with SIV that did not develop lymphomas. This may have set – besides other yet unknown mechanisms – the stage for lymphoma development and might serve as a prognostic marker for *B*-cell tumorigenesis. Lymphoid cytotoxic $CD8^+$ *T* cells, normally acting as tumor antagonists (Jiang et al., 2015), showed signs of exhaustion as indicated by a marked PD-1 upregulation on their cell surface following infection, adding evidence for a compromised immune system that fails to eliminate the tumor. However, in the context of SIV infection expression of PD1 is increased as a result of *T*-cell activation and likely represents an additional activation marker (Hokey et al., 2008; Hong et al., 2013), which fits into the overall picture of an elevated activation status in the two case report animals.

Still, both lymphoma cases differed in certain aspects. First, lymphoma in animal 1 arose at an extranodal as well as a nodal site. It is not clear whether a primary extranodal or a primary nodal NHL development was present in this case. The appearance of a primary extranodal NHL in the stomach with metastasis to the adjacent lymph node is conceivable, but a secondary NHL with first appearance in the lymph node and metastasis to the stomach is also possible.

The gastrointestinal tract (GIT) is the most common extranodal site for NHL, and the stomach represents the most affected organ within the GIT (Chen et al., 2010; Yang et al., 2011; Ding et al., 2016). A primary GIT NHL is rare. Usually, it appears as a secondary tumor (Ghimire et al., 2011). In scientific literature, the definition of primary extranodal NHL is debatable. Krol et al. (2013) subdivided cases of NHL into primary nodal, primary extranodal and NHL with extensive involvement. A correlation between primary extranodal NHL and longer disease-free periods in humans was found (Krol et al., 2003). In our case, it is impossible to trace back the exact chronological development of tumorigenesis, especially since both a nodal as well as an extranodal site in close anatomic proximity were involved.

The immunophenotype of the gastric lymphoma of animal 1 is also debatable. We diagnosed the nodal lymphoma as a classic DLBCL because of the dominant CD20 expression with only minor CD3 staining. As stated in the introduction, DLBCL is the most common type of NHL tumor (Armitage and Weisenburger, 1998). In contrast, levels of CD20 and CD3 expression were similar in the gastric tumor. A minority of CD3 positive cells probably represented pre-existing or recruited non-neoplastic *T* cells. However, the majority of neoplastic cells co-expressed CD3 and CD20. In general, it is not uncommon for *B*-cell lymphomas to co-express *T*-cell markers such as CD2, CD5, CD7 or CD43 (Harris et al., 1994; Inaba et al., 2001). Wang et al. have already described aberrant co-expression of CD3 in four cases of human *B*-cell NHL (Wang et al., 2009). In all these cases, the exact cell origin of the lymphoma was determined by analyzing the rearrangement of *T*-cell receptor and immunoglobulin genes. For future experiments, genotyping of neoplastic cells seems to be inevitable for the correct determination of cell lineage and the genetic relationship between two or more tumors.

Considering the histological features and the equal expression levels of CD3 and CD20, other forms of NHL including the large *B*-cell-rich *T*-cell lymphoma (Higgins et al., 2000) and the *T*-cell/histiocyte-rich large *B*-cell lymphoma (Pittaluga and Jaffe, 2010) were regarded as unlikely differential diagnoses for the gastric tumor.

Animal 2 presented with lymphoma of the DLBCL type located at the urinary bladder neck leading to bilateral urethral obstruction and death due to acute uremia. Lymphoma of the urogenital tract is rare, and a primary extranodal lymphoma in the urinary bladder is even less common (Venyo, 2014). The most common type is the extranodal marginal zone lymphoma of mucosa-associated lymphoid tissue type (MALT lymphoma) and the DLBCL (Bates et al., 2000). The latter develops through transformation of the MALT lymphoma. In an earlier study at our center, just 1 out of 16 SIV-infected rhesus macaques with lymphoma developed a tumor in the urinary bladder (Kahnt et al., 2002).

To summarize, our cases of lymphoma in two SIV-infected rhesus macaques represented special entities regarding either the immunophenotype or localization of the tumor.

5 Conclusions

In conclusion, we correlated the incidence of SIV-associated lymphoma that occurred during the last 25 years at the German Primate Center with the different virus stocks used for infection. Particularly an ex vivo derived SIV, designated SIVmac251/32H/spleen, was associated with a high incidence of lymphoma development which might be due to the presence of an additional pathogen, i.e., the tumorigenic rhLCV, in this virus stock.

Two rhesus macaques with lymphomas developing in the chronic phase of SIV-infection were investigated in more detail in this study. Lymphoma development is a common complication of SIV infection. Both cases revealed unusual characteristics. One animal presented a DLBCL at an extranodal as well as nodal site with co-expression of the *B*-cell marker CD20 and the *T*-cell marker CD3 in the extranodal localization. The other animal revealed an obstructive DLBCL around the urinary bladder neck leading to an unexpected death due to uremia.

6 Data availability

All relevant data are presented in the paper. Please contact the corresponding author for further details.

Author contributions. Antonina Klippert and Martina Bleyer wrote the manuscript with contribution of Maria Daskalaki, Berit Neumann, Ulrike Sauermann and Christiane Stahl-Hennig. Antonina Klippert and Maria Daskalaki collected the samples. Martina Bleyer performed the macroscopical, histological and immunohistochemical examinations. Ulrike Sauermann calculated the incidence and prepared the associated figures and table. Artur Kaul performed the lymphocryptovirus PCR. Antonina Klippert and Berit Neumann analyzed the flow cytometry data. Frank Kirchhoff provided the SIVmac239 *nef* construct. Nicole Stolte-Leeb, Frank Kirchhoff and Christiane Stahl-Hennig prepared and designed the experiment.

Competing interests. The authors declare that they have no conflict of interest.

Acknowledgements. The authors would like to thank Wolfgang Henkel for the assistance during necropsy and Larissa Hummel, Nadine Schminke, Corinna Boike, Judith Hampe, Sandra Heine and Kerstin Eckelmann for excellent laboratory assistance.

Edited by: E. Fuchs
Reviewed by: G. Koopman and one anonymous referee

References

Armitage, J. O. and Weisenburger, D. D.: New approach to classifying non-Hodgkin's lymphomas: clinical features of the major histologic subtypes. Non-Hodgkin's Lymphoma Classification Project, J. Clin. Oncol., 16, 2780–2795, 1998.

Bates, A. W., Norton, A. J., and Baithun, S. I.: Malignant lymphoma of the urinary bladder: a clinicopathological study of 11 cases, J. Clin. Pathol., 53, 458–461, 2000.

Blaschke, S., Hannig, H., Buske, C., Kaup, F. J., Hunsmann, G., and Bodemer, W.: Expression of the simian Epstein-Barr virus-encoded latent membrane protein-1 in malignant lymphomas of SIV-infected rhesus macaques, J. Med. Virol., 65, 114–120, 2001.

Chen, W. L., Tsai, W. C., Chao, T. Y., Sheu, L. F., Chou, J. M., Kao, W. Y., Chen, Y. C., and Ho, C. L.: The clinicopathological analysis of 303 cases with malignant lymphoma classified according to the World Health Organization classification system in a single institute of Taiwan, Ann. Hematol., 89, 553–562, doi:10.1007/s00277-009-0870-z, 2010.

Chmielewicz, B., Goltz, M., Lahrmann, K. H., and Ehlers, B.: Approaching virus safety in xenotransplantation: a search for unrecognized herpesviruses in pigs, Xenotransplantation, 10, 349–356, 2003.

Daniel, M. D., Letwin, N. L., King, N. W., Kannagi, M., Sehgal, P. K., Hunt, R. D., Kanki, P. J., Essex, M., and Desrosiers, R. C.: Isolation of T-cell tropic HTLV-III-like retrovirus from macaques, Science, 228, 1201–1204, 1985.

Ding, W., Zhao, S., Wang, J., Yang, Q., Sun, H., Yan, J., Gao, L., Yao, W., Zhang, W., and Liu, W.: Gastrointestinal Lymphoma in Southwest China: Subtype Distribution of 1,010 Cases Using the WHO (2008) Classification in a Single Institution, Acta Haematol., 135, 21–28, doi:10.1159/000437130, 2016.

Dittmer, U., Stahl-Hennig, C., Coulibaly, C., Nisslein, T., Luke, W., Fuchs, D., Bodemer, W., Petry, H., and Hunsmann, G.: Repeated

exposure of rhesus macaques to low doses of simian immunodeficiency virus (SIV) did not protect them against the consequences of a high-dose SIV challenge, J. Gen. Virol., 76, 1307–1315, doi:10.1099/0022-1317-76-6-1307, 1995.

Fujimoto, K. and Honjo, S.: Presence of antibody to Cyno-EBV in domestically bred cynomolgus monkeys (Macaca fascicularis), J. Med. Primatol., 20, 42–45, 1991.

Ghimire, P., Wu, G. Y., and Zhu, L.: Primary gastrointestinal lymphoma, World J. Gastroenterol., 17, 697–707, doi:10.3748/wjg.v17.i6.697, 2011.

Habis, A., Baskin, G. B., Murphey-Corb, M., and Levy, L. S.: Simian AIDS-associated lymphoma in rhesus and cynomolgus monkeys recapitulates the primary pathobiological features of AIDS-associated non-Hodgkin's lymphoma, AIDS Res. Human Retrov., 15, 1389–1398, doi:10.1089/088922299310098, 1999.

Habis, A., Baskin, G., Simpson, L., Fortgang, I., Murphey-Corb, M., and Levy, L. S.: Rhesus lymphocryptovirus infection during the progression of SAIDS and SAIDS-associated lymphoma in the rhesus macaque, AIDS Res. Human Retrov., 16, 163–171, doi:10.1089/088922200309502, 2000.

Hamilton-Dutoit, S. J., Rea, D., Raphael, M., Sandvej, K., Delecluse, H. J., Gisselbrecht, C., Marelle, L., van Krieken, H. J., and Pallesen, G.: Epstein-Barr virus-latent gene expression and tumor cell phenotype in acquired immunodeficiency syndrome-related non-Hodgkin's lymphoma, Correlation of lymphoma phenotype with three distinct patterns of viral latency, Am. J. Pathol., 143, 1072–1085, 1993.

Harris, N. L., Jaffe, E. S., Stein, H., Banks, P. M., Chan, J. K., Cleary, M. L., Delsol, G., De Wolf-Peeters, C., Falini, B., Gatter, K. C., Grogan, T. M., Isaacson, P. G., Knowles, D. M., Mason, D. Y., Muller-Hermelink, H.-K., Pileri, S. A., Piris, M. A., Ralfkiaer, E., and Warnke, R. A.: A revised European-American classification of lymphoid neoplasms: a proposal from the International Lymphoma Study Group, Blood, 84, 1361–1392, 1994.

Higgins, J. P., van de Rijn, M., Jones, C. D., Zehnder, J. L., and Warnke, R. A.: Peripheral *T*-cell lymphoma complicated by a proliferation of large *B* cells, Am. J. Clin. Pathol., 114, 236–247, doi:10.1309/72CM-KAXF-66DE-4XVA, 2000.

Hokey, D. A., Johnson, F. B., Smith, J., Weber, J. L., Yan, J., Hirao, L., Boyer, J. D., Lewis, M. G., Makedonas, G., Betts, M. R., and Weiner, D. B.: Activation drives PD-1 expression during vaccine-specific proliferation and following lentiviral infection in macaques, Eur. J. Immunol., 38, 1435–1445, doi:10.1002/eji.200737857, 2008.

Hong, J. J., Amancha, P. K., Rogers, K., Ansari, A. A., and Villinger, F.: Re-evaluation of PD-1 expression by *T* cells as a marker for immune exhaustion during SIV infection, PloS one, 8, e60186, doi:10.1371/journal.pone.0060186, 2013.

Inaba, T., Shimazaki, C., Sumikuma, T., and Nakagawa, M.: *T*-cell associated antigen-positive *B*-cell lymphoma, Leuk. Lymphoma, 42, 1161–1171, doi:10.3109/10428190109097741, 2001.

Jiang, Y., Li, Y., and Zhu, B.: *T*-cell exhaustion in the tumor microenvironment, Cell Death Dis., 6, e1792, doi:10.1038/cddis.2015.162, 2015.

Kahnt, K., Matz-Rensing, K., Hofmann, P., Stahl-Hennig, C., and Kaup, F. J.: SIV-associated lymphomas in rhesus monkeys (Macaca mulatta) in comparison with HIV-associated lymphomas, Vet. Pathol., 39, 42–55, 2002.

Klippert, A., Stolte-Leeb, N., Neumann, B., Sauermann, U., Daskalaki, M., Gawanbacht, A., Kirchhoff, F., and Stahl-Hennig, C.: Frequencies of lymphoid *T*-follicular helper cells obtained longitudinally by lymph node fine-needle aspiration correlate significantly with viral load in SIV-infected rhesus monkeys, J. Med. Primatol., 44, 253–262, doi:10.1111/jmp.12186, 2015.

Krol, A. D., le Cessie, S., Snijder, S., Kluin-Nelemans, J. C., Kluin, P. M., and Noordijk, E. M.: Primary extranodal non-Hodgkin's lymphoma (NHL): the impact of alternative definitions tested in the Comprehensive Cancer Centre West population-based NHL registry, Ann. Oncol., 14, 131–139, 2003.

Matz-Rensing, K., Pingel, S., Hannig, H., Bodemer, W., Hunsmann, G., Kuhn, E. M., Tiemann, M., and Kaup, F. J.: Morphologic and immunophenotypic characteristics of malignant lymphomas in SIV-infected rhesus macaques, J. Med. Primatol., 28, 318–328, 1999.

Phillips, K. A., Bales, K. L., Capitanio, J. P., Conley, A., Czoty, P. W., t Hart, B. A., Hopkins, W. D., Hu, S. L., Miller, L. A., Nader, M. A., Nathanielsz, P. W., Rogers, J., Shively, C. A., and Voytko, M. L.: Why primate models matter, Am. J. Primatol., 76, 801–827, doi:10.1002/ajp.22281, 2014.

Pittaluga, S. and Jaffe, E. S.: *T*-cell/histiocyte-rich large *B*-cell lymphoma, Haematologica, 95, 352–356, doi:10.3324/haematol.2009.016931, 2010.

Rivailler, P., Carville, A., Kaur, A., Rao, P., Quink, C., Kutok, J. L., Westmoreland, S., Klumpp, S., Simon, M., Aster, J. C., and Wang, F.: Experimental rhesus lymphocryptovirus infection in immunosuppressed macaques: an animal model for Epstein-Barr virus pathogenesis in the immunosuppressed host, Blood, 104, 1482–1489, doi:10.1182/blood-2004-01-0342, 2004.

Rud, E. W., Cranage, M., Yon, J., Quirk, J., Ogilvie, L., Cook, N., Webster, S., Dennis, M., and Clarke, B. E.: Molecular and biological characterization of simian immunodeficiency virus macaque strain 32H proviral clones containing nef size variants, J. Gen. Virol., 75, 529–543, doi:10.1099/0022-1317-75-3-529, 1994.

Schultheiss, T., Stolte-Leeb, N., Sopper, S., and Stahl-Hennig, C.: Flow cytometric characterization of the lymphocyte composition in a variety of mucosal tissues in healthy rhesus macaques, J. Med. Primatol., 40, 41–51, doi:10.1111/j.1600-0684.2010.00446.x, 2011.

Siddiqui, R. A., Sauermann, U., Altmuller, J., Fritzer, E., Nothnagel, M., Dalibor, N., Fellay, J., Kaup, F. J., Stahl-Hennig, C., Nurnberg, P., Krawczak, M., and Platzer, M.: X chromosomal variation is associated with slow progression to AIDS in HIV-1-infected women, Am. J. Hum. Genet., 85, 228–239, doi:10.1016/j.ajhg.2009.07.013, 2009.

Swerdlow, S. H., Campo, E., Hariis, N. L., Jaffe, E. S., Pileri, S. A., and Stein, H., Thiele, J., and Vardiman, J. W.: WHO classification of tumours of haematopoetic and lymphoid tissues, in: WHO classification of tumours of haematopoetic and lymphoid tissues, IARC, 439 pp., 2008.

Venyo, A. K.: Lymphoma of the urinary bladder, Adv. Urol., 2014, 327917, doi:10.1155/2014/327917, 2014.

Wang, F.: Nonhuman primate models for Epstein-Barr virus infection, Curr. Opin. Virol., 3, 233–237, doi:10.1016/j.coviro.2013.03.003, 2013.

Wang, J., Chen, C., Lau, S., Raghavan, R. I., Rowsell, E. H., Said, J., Weiss, L. M., and Huang, Q.: CD3-positive large *B*-cell lymphoma, Am. J. Surg. Pathol., 33, 505–512, doi:10.1097/PAS.0b013e318185d231, 2009.

Yang, Q. P., Zhang, W. Y., Yu, J. B., Zhao, S., Xu, H., Wang, W. Y., Bi, C. F., Zuo, Z., Wang, X. Q., Huang, J., Dai, L., and Liu, W. P.: Subtype distribution of lymphomas in Southwest China: analysis of 6,382 cases using WHO classification in a single institution, Diagn. Pathol., 6, 77, doi:10.1186/1746-1596-6-77, 2011.